How to cite: *Angew. Chem. Int. Ed.* **2021**, *60*, 11158–11162
International Edition: doi.org/10.1002/anie.202100054
German Edition: doi.org/10.1002/ange.202100054

Prodrugs

An Endoplasmic Reticulum Specific Pro-amplifier of Reactive Oxygen Species in Cancer Cells

*Hong-Gui Xu, Margot Schikora, Miroslav Sisa, Steffen Daum, Insa Klemt, Christina Janko, Christoph Alexiou, Galyna Bila, Rostyslav Bilyy, Wenjie Gong, Michael Schmitt, Leopold Sellner, and Andriy Mokhir**

Abstract: *The folding and export of proteins and hydrolysis of unfolded proteins are disbalanced in the endoplasmic reticulum (ER) of cancer cells, leading to so-called ER stress. Agents further augmenting this effect are used as anticancer drugs including clinically approved proteasome inhibitors bortezomib and carfilzomib. However, these drugs can affect normal cells, which also rely strongly on ER functions, leading, for example, to accumulation of reactive oxygen species (ROS). To address this problem, we have developed ER-targeted prodrugs activated only in cancer cells in the presence of elevated ROS amounts. These compounds are conjugates of cholic acid with N-alkylaminoferrocene-based prodrugs. We confirmed their accumulation in the ER of cancer cells, their anticancer efficacy, and cancer cell specificity. These prodrugs induce ER stress, attenuate mitochondrial membrane potential, and generate mitochondrial ROS leading to cell death via necrosis. We also demonstrated that the new prodrugs are activated in vivo in Nemeth-Kellner lymphoma (NK/Ly) murine model.*

According to estimation of European Cancer Information System (ECIS) in the European Union 1.3 millions of people will die from cancer and over 2.7 million of new cases (excluding non-melanoma skin cancer) will be diagnosed in 2020.[1] Treatment of this disease is complicated, since cancer and normal cells are related and, correspondingly, precise targeting/killing of the former cells without affecting of the latter ones is a challenging and not yet fully solved problem. In particular, currently available, clinically approved chemotherapeutics exhibit dose-limiting side effects, which adversely and sometimes irreversibly affect the quality of life of patients.[2] Cancer cells can be addressed specifically by making use of their unique features, for example, the presence of some overexpressed receptors,[3] altered glycolysis,[4] and elevated amounts of reactive oxygen species ($ROS = H_2O_2$, $O_2^{\bullet-}$ and $HO^{\bullet}$).[5,6] The endoplasmic reticulum (ER) has been recognized as an especially attractive target due to the following reasons.[7] In cancer cells the balance between folding/transport of proteins and degradation of misfolded proteins is disturbed that leads to the so called ER stress. Further potentiation of the stress by chemical agents induces cancer cell death, whereas normal cells initially lacking the ER stress withstand the drug effect. Though some cancer cell selectivity can be achieved, side effects are also expected. They include, but not limited to induction of moderate ER stress in normal cells leading to unfolded protein response (UPR), elevation of intracellular amounts of ROS and disbalance of Ca^{2+} homeostasis. All these factors contribute to genome instability that stimulate carcinogenesis.[8]

Herein we addressed this problem by the development of ER targeting prodrugs **4a-g**, which are activated only in cancer cells, but remain inactive in normal cells (Scheme 1, Scheme 2). These compounds are based on N-substituted aminoferrocene (AF) drugs. After their formation in cells these drugs cycle between reduced (AF) and oxidized (AF^+) forms catalyzing the formation of highly reactive ROS $O_2^{\bullet-}$ (from O_2) and $HO^{\bullet}$ (from H_2O_2) that leads to cell death.[9]

[*] M. Sc. H.-G. Xu, M. Sc. M. Schikora, Dr. M. Sisa, Dr. S. Daum, M. Sc. I. Klemt, Prof. Dr. A. Mokhir
Friedrich-Alexander University Erlangen-Nürnberg (FAU)
Department of Chemistry and Pharmacy
Organic Chemistry Chair II
Nikolaus-Fiebiger-Str. 10, 91058 Erlangen (Germany)
E-mail: Andriy.Mokhir@fau.de

Dr. M. Sisa
Institute of Experimental Botany AS CR
Prague (Czech Republic)

Dr. C. Janko, Prof. Dr. C. Alexiou
Else Kröner-Fresenius-Stiftung-Professorship
Department of Otorhinolaryngology, Head and Neck Surgery
Section of Experimental Oncology and Nanomedicine (SEON)
Universitätsklinikum Erlangen
Glückstraße 10a, 91054 Erlangen (Germany)

M. Sc. G. Bila, Prof. Dr. R. Bilyy
Danylo Halytsky Lviv National Medical University
Pekarska str. 69, 79010 Lviv (Ukraine)

Dr. W. Gong, Prof. Dr. M. Schmitt, Dr. L. Sellner
Department of Medicine V, Heidelberg University Hospital
Im Neuenheimer Feld 410, 69120 Heidelberg (Germany)

Dr. W. Gong
Hematology Department
First Affiliated Hospital of Soochow University, Suzhou (China)

Dr. L. Sellner
Takeda Pharma Vertrieb GmbH & Co. KG
Jägerstr. 27, 1017 Berlin (Germany)

Supporting information and the ORCID identification number for one of the authors of this article can be found under: https://doi.org/10.1002/anie.202100054.

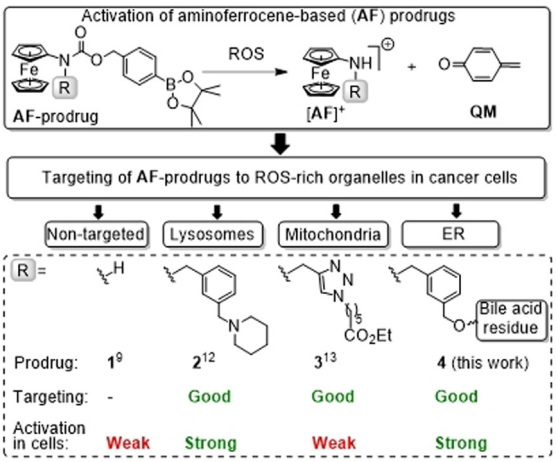

Scheme 1. The mechanism of activation of AF-based prodrugs and state-of-the-art in the targeting of these prodrugs to organelles in cancer cells.

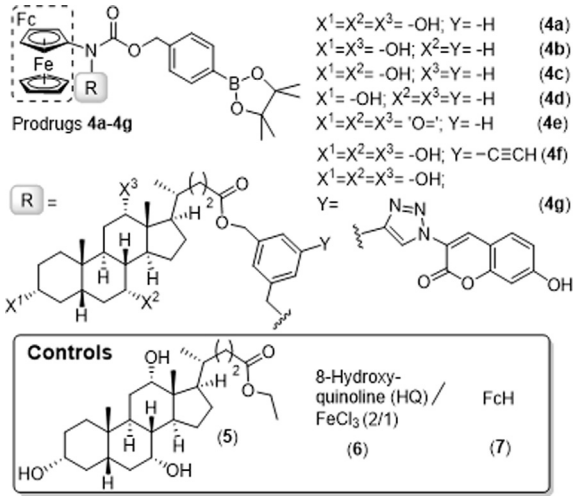

Scheme 2. Structures of AF prodrugs targeting ER (**4a**–**g**) and control compounds.

These and other ferrocene-based biologically active compounds were described in several recent reviews.[10] The AF′s are protected in prodrugs **4** with a 4-(carbonyloxymethyl)-phenylboronic acid pinacol ester group.[9] The latter group is labile under oxidative conditions and was, therefore, expected to be cleaved especially well within the ER of cancer cells, which is known to have more oxidative environment than the cytoplasm.[11]

Our research group has substantial experience with AF-based prodrugs. We have previously investigated their mode of action[9,12] and developed compounds targeting lysosomes (LY)[13] and mitochondria (Mit)[14] in cancer cells (Scheme 1). However, ER specific AF-prodrugs were not available before this work. P. Cloetens, G. Jaouen and S. Bohic have recently reported on anticancer osmocenyl-tamoxifen prodrugs, which are accumulated in endomembrane system of breast cancer MDA-MB-231 cells including, apart from ER, nuclear envelope, endosomes and lysosomes.[15] Another example of an ER-targeting prodrug is disulfiram. Its mode of action relies on the activation by binding of Cu ions in cells. Apart from inducing ER stress via proteasome inhibition and ROS production,[16] it affects other targets including inhibition of aldehyde dehydrogenase (ALDH) and the STAT3 signaling pathway,[17] modulation of DNA-topoisomerases and methyltransferases as well as glutathione S-transferase.[18] Thus, the known anticancer prodrugs are not ER specific.

Previously reported ER-carriers are usually hydrophobic structures, for example, cyanine dye DiOC6, hexyl rhodamine B, polyethylene glycol (PEG), long alkyl chains, derivatives of p-methylphenylsulfonamides.[19] Since water solubility of AF-prodrugs is limited (≤ 50 μM),[9,12–14] their further modification with the known ER-carriers would with high probability lead to non-soluble in water compounds. Therefore, we searched for alternative modifiers. We selected bile acids, since along with their hydrophobic core, they carry polar groups (alcohol or carbonyl), which could provide for water solubility. To find the best modifier, we introduced a series of bile acid fragments (substituent R, Scheme 2) to obtain prodrugs **4a**–**4e** as described in the supporting information (*SI*). We were pleased to observe that all prepared prodrugs are soluble at least up to 50 μM in aqueous solution (Table S1, *SI*). All prodrugs affect the viability of Burkitt's lymphoma BL-2 cells (Table S2, *SI*), selected as a representative cancer cell line. Derivatives of cholic (**4a**, $IC_{50} = 9 \pm 2$ μM) and dehydrocholic acid (**4e**, $IC_{50} = 9 \pm 2$ μM) are most potent in this series. They exhibit a stronger anticancer effect than the non-targeted control **1**[9] ($IC_{50} = 34 \pm 3$ μM, $p < 0.001$) and the Mit-targeting prodrug **3**[14] ($IC_{50} = 35 \pm 2$ μM, $p < 0.001$) reaching the potency of the best previously reported LY-targeting prodrug **2**[13] ($IC_{50} = 5 \pm 2$ μM). Based on these data and due to its easier synthesis, prodrug **4a** was selected for more detailed studies.

As previously established, prodrugs containing arylboronic acid pinacol ester are hydrolyzed in aqueous buffered at pH 7 solutions within ≤ 1 h.[20] Therefore, the active form of **4a** will be the boronic acid **4a**_BA. We determined n-octanol/water partition coefficient (logP) of **4a**_BA to be substantially higher (5.9 ± 0.2, Table S3, *SI*) than that of parent prodrug **1**_BA (2.7 ± 0.2). The high lipophilicity of **4a**_BA was expected to facilitate its accumulation in the ER.[19]

To investigate the mechanism of **4a** activation in the presence of H_2O_2, we applied electrospray ionization (ESI) mass spectrometry (MS). We confirmed that **4a** is first hydrolyzed in aqueous solution forming **4a**_BA. In the presence of H_2O_2 AF-drug **4a_2** is formed (Figures S29–S34, *SI*), which can donate an electron to H_2O_2/O_2 leading to formation of ferrocenium **4a_2**$^+$ and highly toxic $HO^{\bullet}/O_2^{\bullet-}$. We confirmed experimentally formation of $HO^{\bullet}/O_2^{\bullet-}$ in mixtures of **4a** and H_2O_2 by using 2′,7′-dichlorodihydrofluorescein (DCFH) (Figure S35, Table S4, *SI*). In particular, we found that **4a** accelerates the rate of DCFH oxidation by 3.2-fold with respect to the rate of its spontaneous oxidation by H_2O_2. All together these data indicate that **4a** is activated as outlined in Scheme 1 similarly to other known AF-prodrugs.[9,12–14]

Further, we confirmed that apart from BL-2 cells prodrug **4a** exhibits anticancer activity towards other cancer cell lines including ovarian cancer A2780 ($IC_{50} = 5.4 \pm 0.7$ μM) and T-

cell leukemia Jurkat ($IC_{50} = 18 \pm 1\ \mu M$). The anticancer activity of LY-targeting prodrug **2**[13] is similar towards A2780 cells ($IC_{50} = 7 \pm 2\ \mu M$) and higher towards Jurkat cells ($IC_{50} = 7.2 \pm 0.1\ \mu M$, $p < 0.001$), whereas that of Mit-targeting **3**[14] is substantially lower for both cell lines ($p < 0.001$, Tables S5, S6, *SI*). For Jurkat cells we observed that **4a** induces cell death mainly via necrosis and partially via apoptosis (Figure S36A, *SI*) that was reproduced for A2780 cells (Figure S37, *SI*). Since necrotic cells are usually immunogenic, it is possible that the initial direct anticancer effect of **4a** will be facilitated by the action of immune system in vivo. We observed that the anticancer activity of **4a** in Jurkat cells is decreased in the presence of the ROS inhibitor N-acetylcysteine (NAC)[21] (Figure S36B, *SI*). These data confirm that ROS is involved in the intracellular activation of **4a**.

Next, we investigated the mechanism of action of **4a** in cells. In the first experiment, we incubated A2780 cells with prodrug **4a** as well as controls **1** and **2** for time periods between 1–24 h followed by their staining with organelle-specific dyes (ER: ER-tracker-green, ERTgrn; LY: acridine orange, AO; Golgi: Golgi-Staining-Green, GO; Mit: rhodamine 123, R123) and evaluation of their fluorescence by using flow cytometry (Figure 1). The fluorescence intensity of the cells treated with medium only (carrier) was used as a reference. We observed that non-targeted control **1** weakly affects the ER-specific fluorescence at 1 h incubation (but not at 4 h incubation) and does not affect the LY-, Golgi- and Mit-specific fluorescence at both 1 and 4 h incubation times. A weak decrease of the Mit-specific fluorescence was observed at the highest incubation time of 24 h. As expected, LY-targeted **2** strongly reduces the LY-specific fluorescence of the cells. Additionally, it also affects ER and especially Mit that can be a follow up effect after the initial lysosomal disruption as previously reported.[13] The effect of **4a** on the ER-specific fluorescence of the cells for both 1 and 4 h incubation times was found to be strongest within the studied series of the prodrugs ($p < 0.001$, Figure 1 A). Using confocal microscopy we observed that the ER tracker dye is leaking into the nuclei and the cytoplasm of a large proportion of **4a**-treated cells indicating that **4a** induces the ER disruption (Figure S38). In contrast to **2**, prodrug **4a** does not affect the LY-specific signal (Figure 1 B), but at the early incubation time (1 h) decreases slightly the Golgi-specific fluorescence and does not affect the Mit-specific fluorescence. At the later incubation times the effects on Golgi and Mit become stronger. These data indicate that the ER is a primary site of action for **4a** (the strong effect is seen already at 1h-incubation), whereas the effects on Golgi and Mit are secondary (≥ 4 h incubation is needed to observe strong effects).

By using quantitative PCR, we observed that the expression of mRNA of CCAAT-enhancer-binding protein homologous protein (CHOP), which is a marker of the ER stress,[22] is significantly increased in **4a**-treated A2780 cells ($p < 0.05$). In contrast, neither unspecific **1** nor LY-targeting **2** affected the expression of the CHOP-mRNA (Table S7, *SI*). These data indicate that **4a** exhibits its anticancer activity via the induction of the ER stress.

Next, we evaluated the ability of **4a** to modulate the oxidative stress in cells (Figure 2 A,B). We observed that this prodrug increases the total intracellular ROS amount (tROS)

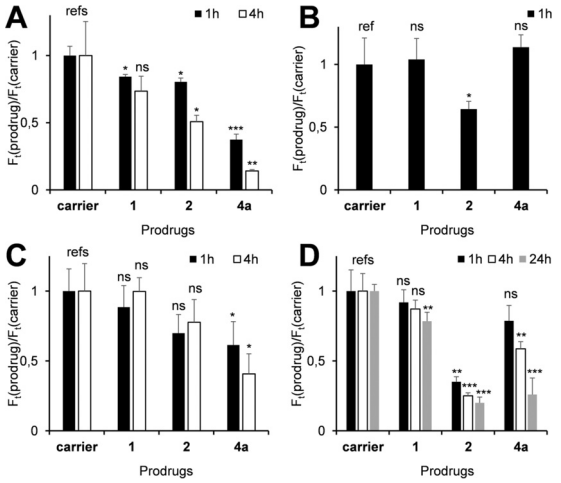

Figure 1. Effect of prodrugs and controls on relative organelle-specific staining (F_t(prodrug)/F_t(carrier)), where F is emission at 525 nm ($\lambda_{ex} = 488$ nm). Incubation times with prodrugs (1, 4, or 24 h) are indicated on the plots. A) ER staining with ERTgrn. B) LY staining with AO. C) Golgi staining with GO. D) Mit staining with R123. References are indicated with "ref". The experimental data were compared by using Student's t test: $p < 0.05$ (*), $p < 0.01$ (**), $p < 0.001$ (***), $p \geq 0.05$ (ns).

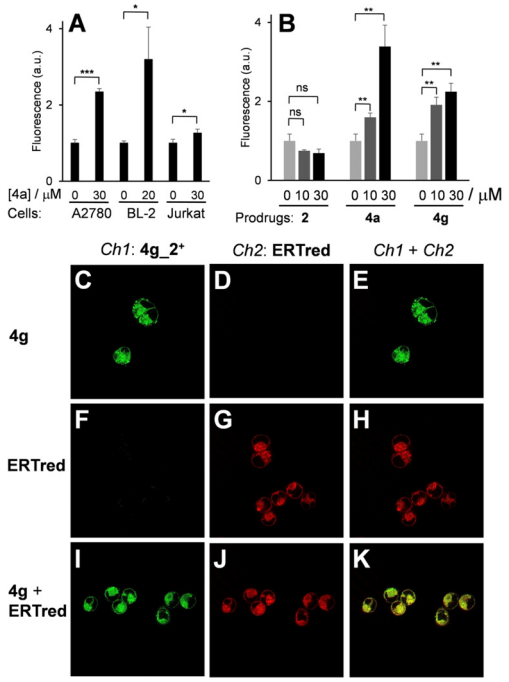

Figure 2. A) Increase of the mean fluorescence ($\lambda_{ex} = 488$ nm, $\lambda_{em} = 530$ nm) of 5-(6-)chloromethyl-2′,7′-dichlorodihydrofluorescein diacetate (CM-DCFH-DA)-loaded cells incubated with **4a** for 2 h (A2780 and BL-2 cells) or 1 h (Jurkat cells). B) Increase of the mean fluorescence ($\lambda_{ex} = 488$ nm, $\lambda_{em} = 585$ nm) of A2780 cells incubated with **4a** for 2 h followed by Mitosox™ for 20 min. C–K) Images of A2780 cells stained with **4g** (C–E), ERTred (F–H), and a mixture of **4g** and ERTred (I–K). Fluorescent channels: *Ch1* (green)—λ_{ex}: 335–383 nm; λ_{em}: 420–470 nm (detection of **4g_2**$^+$); *Ch2* (red)—λ_{ex}: 538–562 nm; λ_{em}: 570–640 nm (detection of ERTred).

in all studied cell lines significantly. However, the overall magnitude of the tROS increase was substantially lower than that found for LY-targeting **2**.[13] In contrast, we observed the strong dose-dependent increase of mitochondrial ROS (mROS) in A2780 cells treated with **4a**, whereas control **2** did not affect mROS at any concentration tested (0–30 μM). Thus, the mode of action of **4a** (the induction of ER stress, the increase of mROS) is distinct from that implicated for all previously known AF-prodrugs.[9,12–14,20]

To find out whether **4a** is directly accumulated in ER or induces its effects on the ER indirectly, we prepared its fluorogenic analogue **4g** containing a fluorescent dye 7-hydroxycoumarine (*SI*). We confirmed that **4g** and **4a** are analogues. For example, they have similar solubility in aqueous solution (Table S1, *SI*), lipophilicity (Table S3, *SI*) and exhibit similar anticancer activity towards A2780 cells ($IC_{50} = 6.2 \pm 2.4$ vs. $IC_{50} = 5.4 \pm 0.7$ μM correspondingly).

Prodrug **4g** is practically not fluorescent due to photo-induced electron transfer (PET) from the ferrocene moiety to the dye. Analogously to **4a**, it is converted to AF-drug **4g_2**$^+$ in the presence of H_2O_2 (Figure S29, S30) that is accompanied by the strong (up to 50-fold) fluorescence increase (Figure S39). We found that **4g** is accumulated and activated in A2780 cells leading to formation of fluorescent products (most probably **4g_2**$^+$) that could be monitored by flow cytometry (Figure S40, Table S9). By using fluorescence microscopy we confirmed that the fluorescent product derived from **4g** is accumulated in ER (Figure 2C–K). This is evident from the efficient overlap (Pearson's R value = 0.85, Figure S41, *SI*) of the signal of the fluorescent product **4g_2**$^+$ derived from **4g** (green color) and the signal of ER-specific stain ERTred (red color, Figure 2K). It should be mentioned that previously reported fluorogenic versions of LY-targeting **2**[13] and Mit-targeting **3**[14] are substantially less active than their unlabeled counterparts. These compounds are suitable for the study of the mechanism of prodrug action, but not as therapeutic agents. In contrast, **4g** is the first truly teranostic AF-based prodrug.

To evaluate the cancer cell specificity of the ER-targeting AF-prodrugs, we conducted two complementary experiments. For the first one we selected a pair of genetically related primary cancer (chronic lymphocytic leukemia: CLL) and normal cells (mononuclear cells: MNC's). MNC's is a mixture of cells containing primary B cells, which are parent for CLL cells. We observed that **4a** is significantly more toxic towards CLL cells ($IC_{50} = 5.6 \pm 0.7$ μM) than normal MNC's ($IC_{50} = 18.3 \pm 7.5$ μM, $p < 0.05$) (Figure S42, *SI*). Furthermore, by using fluorescence microscopy we confirmed that **4g** (the fluorogenic analogue of **4a**) is activated only in cancer (A2780), but not in normal (SBLF9 fibroblasts) cells (Figure S43, *SI*). We selected the SBLF9 cells as representative normal cells, since they are adherent and, therefore, better suitable for the fluorescence microscopy than the non-adherent MNC's.

Finally, we evaluated the activation of **4g** in vivo in C57/BL6N mice with Nemeth-Kellner lymphoma (NK/Ly), which grow in the form of ascites (*SI*). First, we took ascite probes from untreated mice (time point 0) as a reference. Then prodrug **4g** at the dose of 40 mg kg^{-1} was injected i.p. every

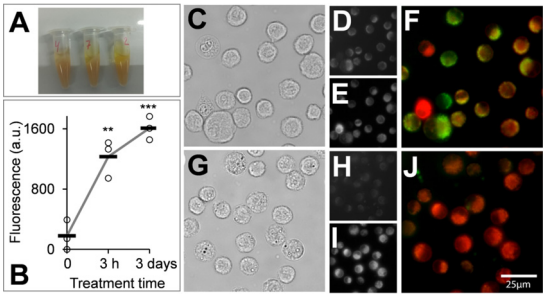

Figure 3. A) Photograph of ascite suspensions isolated from C57/BL6N mice carrying NK/Ly and treated with **4g** for 3 days. B) Increase of the mean fluorescence (λ_{ex} = 340–380 nm; λ_{em} = 435–485 nm) of ascites isolated from the C57/BL6N mice treated with **4g** for 0, 3 h and 3 days: circles: individual data, horizontal bars: means of the individual data. Student's t test: ** – $p < 0.01$; *** – $p < 0.001$; the untreated sample was used as a reference. C) Bright-field images of ascites isolated from the C57/BL6N mice treated with **4g** for 3 days. D, E) Fluorescence image of the same cells as in (C): λ_{ex} = 290–410 nm; λ_{em} = 415–465 nm (D) and λ_{ex} = 530–570 nm; λ_{em} = 570–650 nm (E). F) Overlay of images shown in (D) (green color) and (E) (red color). G–J) Controls; the same as (C–F) for untreated ascites.

day for 3 days. Ascite probes were taken 3 h and 3 days after the beginning of the treatment. The cell suspensions appeared yellow indicating the prodrug uptake (Figure 3A). Furthermore, the fluorescence of ascites (λ_{ex} = 360/20 nm, λ_{ex} = 460/25 nm) was quantified by using a fluorescence plate reader (*SI*). We observed the significant ($p < 0.01$ for 3 h incubation and $p < 0.001$ for 3 days incubation) time-dependent fluorescence increase in the treated animals compared to the non-treated ones (Figure 3B) that is in agreement with the activation of **4g** in vivo. These results were confirmed by imaging of the live ascites by using vital fluorescence microscopy (3 days incubation, Figure 1C–J). In particular, we imaged the cells at two settings (Ch1 and Ch2), which allowed detecting the products of **4g** activation (Ch1: λ_{ex} = 290–410 nm; λ_{em} = 415–465 nm) and the ER-tracking dye ERTred (Ch2: λ_{ex} = 530–570 nm; λ_{em} = 570–650 nm, added to the isolated ascites shortly before the measurements). For the ascites from the treated group we observed an intense signal in the Ch1 indicating the **4g** activation. The latter signal overlaps with that in the Ch2 indicating that **4g** is accumulated and activated in the ER of the ascites in vivo. As expected, no signal in the Ch1 was observed in the ascites isolated from the control (untreated) group. These data are in agreement with our in vitro studies (Figure 2C–K).

In summary, we successfully prepared cholic acid-conjugated AF- prodrug **4a** as well as its fluorogenic version **4g**, which is the first reported teranostic AF-prodrug. We demonstrated fast (≤ 1 h incubation) accumulation and activation of these prodrugs in the ER of cancer cells that leads to the significant ER stress (upregulation of CHOP-mRNA) and the production of both mitochondrial and total ROS. We have confirmed the excellent cancer cell specificity of prodrugs **4a**/**4g** and demonstrated that **4g** is efficiently activated in vivo in the NK/Ly murine model. The prodrugs **4a**/**4g** described in this paper and the previously reported LY-targeting **2**[13] exhibit comparable anticancer effects. However, due to different mechanisms of action, these drugs are

complementary to each other. We assume that **4a**/**4g** may find applications in cases when **2** is not suitable. Furthermore, the simultaneous use of these prodrugs would be an interesting option due to the possible synergistic effects between them.

Acknowledgements

Leonard Mach has conducted preliminary studies, which were not included in this publication. This project has received funding from the German Research Council (DFG, MO1418/7-2) and the European Union's Horizon 2020 research and an innovation program FET Open under grant agreement No 861878 (project "NeutroCure"). C.A. acknowledges funding from Manfred Roth-Stiftung, Fürth, the Forschungsstiftung Medizin am Universitsätsklinikum Erlangen (Germany) and Hans Wormser, Herzogenaurach (Germany). Confocal microscopy was conducted at the Optical Imaging Centre Erlangen (OICE). Open access funding enabled and organized by Projekt DEAL.

Conflict of interest

The authors declare no conflict of interest.

Keywords: aminoferrocene · cancer · endoplasmic reticulum · prodrugs · reactive oxygen species

[1] ECIS—European Cancer Information System: from https://ecis.jrc.ec.europa.eu, accessed on 25/08/2020© European Union, **2020**.
[2] V. Schirrmacher, *Int. J. Oncol.* **2019**, *54*, 407 – 419.
[3] T. Vu, F. X. Claret, *Front. Oncol.* **2012**, *2*, 62.
[4] a) W. H. Koppenol, P. L. Bounds, C. V. Dang, *Nat. Rev. Cancer* **2011**, *11*, 325 – 337; b) O. Warburg, *Science* **1956**, *123*, 309 – 314.
[5] F. Antunes, R. Cadenas, *FEBS Lett.* **2000**, *475*, 121 – 126.
[6] a) T. P. Szatrowski, C. F. Nathan, *Cancer Res.* **1991**, *51*, 794 – 798; b) B. Halliwell, *Biochem. J.* **2007**, *401*, 1 – 11.
[7] A. P. King, J. J. Wilson, *Chem. Soc. Rev.* **2020**, *49*, 8113 – 8136.
[8] N. Siwecka, W. Rozpędek, D. Pytel, A. Wawrzynkiewicz, A. Dziki, Ł. Dziki, J. A. Diehl, I. Majsterek, *Int. J. Mol. Sci.* **2019**, *20*, 4354.
[9] S. Daum, V. Chekhun, I. Todor, N. Lukianova, Y. Shvets, L. Sellner, K. Putzker, J. Lewis, T. Zenz, I. Graaf, G. Groothuis, A. Casini, O. Zozulia, F. Hampel, A. Mokhir, *J. Med. Chem.* **2015**, *58*, 2015 – 2024.
[10] a) S. Peter, B. A. Aderibigbe, *Molecules* **2019**, *24*, 3604; b) M. Patra, G. Gasser, *Nat. Rev. Chem.* **2017**, *1*, 0066.
[11] C. Hwang, A. J. Sinskey, H. F. Lodish, *Science* **1992**, *257*, 1496 – 1502.
[12] S. Daum, S. Babiy, H. Konovalova, W. Hofer, A. Shtemenko, N. Shtemenko, C. Janko, C. Alexiou, A. Mokhir, *J. Inorg. Biochem.* **2018**, *178*, 9 – 17.
[13] S. Daum, V. Reshetnikov, M. Sisa, T. Dumych, M. D. Lootsik, R. Bilyy, E. Bila, C. Janko, A. Alexiou, M. Herrmann, L. Sellner, A. Mokhir, *Angew. Chem. Int. Ed.* **2017**, *56*, 15545 – 15549; *Angew. Chem.* **2017**, *129*, 15751 – 15755.
[14] a) V. Reshetnikov, S. Daum, C. Janko, W. Karawacka, R. Tietze, C. Alexiou, S. Paryzhak, T. Dumych, R. Bilyy, P. Tripal, B. Schmid, R. Palmisano, A. Mokhir, *Angew. Chem. Int. Ed.* **2018**, *57*, 11943 – 11946; *Angew. Chem.* **2018**, *130*, 12119 – 12122; b) V. Reshetnikov, H. G. Özkan, S. Daum, C. Janko, C. Alexiou, C. Sauer, M. R. Heinrich, A. Mokhir, *Molecules* **2020**, *25*, 2545.
[15] F. Fus, Y. Yang, H. Z. S. Lee, S. Top, M. Carriere, A. Bouron, A. Pacureanu, J. Cesar da Silva, M. Salmain, A. Vessières, P. Cloetens, G. Jaouen, S. Bohic, *Angew. Chem. Int. Ed.* **2019**, *58*, 3461 – 3465; *Angew. Chem.* **2019**, *131*, 3499 – 3503.
[16] a) D. Chen, Q. C. Cui, H. Yang, Q. P. Dau, *Cancer Res.* **2006**, *66*, 10425 – 10433; b) K. Butcher, V. Kannappan, R. S. Kilari, M. R. Morris, C. McConville, A. L. Armesilla, W. Wang, *BMC Cancer* **2018**, *18*, 753.
[17] Q. Yang, Y. Yao, K. Li, L. Jiao, J. Zhu, C. Ni, M. Li, Q. P. Dou, H. Yang, *Curr. Pharm. Des.* **2019**, *25*, 3248 – 3256.
[18] E. Ekinci, S. Rohondia, R. Khan, Q. P. Dou, *Recent Pat. Anti-Cancer Drug Discovery* **2019**, *14*, 113 – 132.
[19] P. Gao, W. Pan, N. Li, B. Tang, *Chem. Sci.* **2019**, *10*, 6035 – 6071.
[20] S. Daum, J. Toms, V. Reshetnikov, H. G. Özkan, F. Hampel, S. Maschauer, A. Hakimioun, F. Beierlein, L. Sellner, M. Schmitt, O. Prante, A. Mokhir, *Bioconjugate Chem.* **2019**, *30*, 1077 – 1086.
[21] S. Y. Sun, *Cancer Biol. Ther.* **2010**, *9*, 109 – 110.
[22] S. Oyadomari, M. Mori, *Cell Death Differ.* **2004**, *11*, 381 – 389.

Manuscript received: January 3, 2021
Accepted manuscript online: March 3, 2021
Version of record online: April 8, 2021

